Eur. Phys. J. B **36**, 511–518 (2003)
DOI: 10.1140/epjb/e2004-00006-4

THE EUROPEAN PHYSICAL JOURNAL B

Magnetic order in RCr_2Si_2 intermetallics

O. Moze[1,a], M. Hofmann[2], J.M. Cadogan[3], K.H.J. Buschow[4], and D.H. Ryan[5]

[1] INFM, Unità di Modena, Dipartimento di Fisica, Università di Modena e Reggio Emilia, Via G. Campi 213/a, 41100 Modena, Italy
[2] FRM-II, Technische Universität München, 85747, Garching, Germany
[3] School of Physics, University of New South Wales, Sydney, NSW 2052, Australia
[4] Van der Waals-Zeeman Institute, University of Amsterdam, Valckenierstraat 65, 1018 XE, The Netherlands
[5] The Centre for the Physics of Materials and the Physics Department, McGill University, 3600 University St., Montreal (Quebec), H3A 2T8, Canada

Received 4 November 2003
Published online 30 January 2004 –

Abstract. The magnetic structure and ordering temperatures of three intermetallic compounds which crystallize in the tetragonal $ThCr_2Si_2$ structure, $TbCr_2Si_2$, $HoCr_2Si_2$ and $ErCr_2Si_2$, have been determined by neutron diffraction, differential scanning calorimetry and magnetization measurements. The Cr-sublattice orders anti-ferromagnetically with Néel temperatures of 758 K for $TbCr_2Si_2$, 718 K for $HoCr_2Si_2$ and 692 K for $ErCr_2Si_2$. Chromium atoms located at 4d crystallographic sites are aligned anti-parallel along the c-axis, with G_ZCr magnetic modes. In contrast with metallic bcc Cr, the refined room temperature value of the ordered Cr moment is anomalously large for all three compounds. No long range magnetic order of the R sublattice in $TbCr_2Si_2$ and $HoCr_2Si_2$ is observed, whilst the Er sublattice in $ErCr_2Si_2$ orders independently of the Cr sublattice below 2.4 K with moments ferromagnetically aligned in the basal plane.

PACS. 75.25.+z Spin arrangements in magnetically ordered materials (including neutron and spin-polarized electron studies, synchrotron-source X-ray scattering, etc.) – 75.30.Cr Saturation moments and magnetic susceptibilities – 75.50.Ee Antiferromagnetics

1 Introduction

Compounds which crystallize in the tetragonal ternary silicide $ThCr_2Si_2$ and equivalent $CeAl_2Ge_2$ structure (Space Group I4/mmm) display an enormous variety of magnetic phenomena [1] with hundreds of rare earth intermetallic compounds crystallizing in this extremely important structure type [2,3]. The compound $ThMn_2Si_2$, for example, orders anti-ferromagnetically, with a Néel temperature of 483 K [4] and intermetallics of the type RMn_2Si_2 have been of particular interest, since numerous neutron diffraction investigations clearly prove that the Mn sublattice orders anti-ferromagnetically below 500 K [5]. On the other hand, RT_2Si_2 compounds (with T = Fe, Ni, Co) have been classified as weak Pauli paramagnets, where only the rare earth sublattice orders magnetically and the T sublattice is known not to order magnetically [6]. Bulk magnetization data reported for the series RCr_2Si_2 (R = Gd, Tb, Dy, Ho, Er, and Tm) indicate that the R ions in this series order only at low cryogenic temperatures and that the ordering temperatures scale approximately with the de Gennes factor [7]. The large variety of magnetic phenomena observed in this structure type is due to the dependence of the RKKY exchange interaction on inter- and intra-planar distances. The crystal electric field interaction at the R site in the series RT_2Si_2, generated by a square prism of eight Si atoms and eight almost equidistant T atoms, is an additional source to the magnetic phenomena displayed in this series. Since these two atoms can present a large variation in their electronic properties, an equally large variation in the concomitant magnetic properties of the RT_2Si_2 compounds can be expected. Self-consistent band structure calculations of the valence electron contribution to the EFG (Electric Field Gradient) at the R site and experimental determinations of the EFG demonstrate that the 2nd order crystal field coefficient A_2^0 changes sign when passing from RCr_2Si_2, RFe_2Si_2, RNi_2Si_2 compounds ($A_2^0 > 0$) to RCu_2Si_2 compounds ($A_2^0 < 0$) [8,9]. An inelastic neutron scattering investigation of the crystal field interaction in $HoCr_2Si_2$ has confirmed this predicted sign change in RCr_2Si_2 compounds [10].

[a] e-mail: moze.oscar@unimore.it

Magnetization measurements on the mixed series $RFe_{2-x}Cr_xSi_2$ demonstrated the presence of antiferromagnetic interactions for Cr-rich compounds with ordering temperatures up to 700 K, whilst low ordering temperatures were observed for Fe rich compounds [11]. This led us to investigate whether or not the Cr sublattice is in fact magnetic in the RCr_2Si_2 series. Magnetic ordering of the Cr sublattice at low temperatures (1.6−293 K) was indeed observed directly by neutron diffraction for the first time in a prototypical compound of the $ThCr_2Si_2$ structure, $HoCr_2Si_2$ [12]. Prior to this, no definitive neutron diffraction studies had been reported for the RCr_2Si_2 series. Here, we report important new details on the magnetic structures of the Cr and R sublattices in the compounds $TbCr_2Si_2$, $HoCr_2Si_2$ and $ErCr_2Si_2$, investigated by neutron powder diffraction, DSC (Differential Scanning Calorimetry) and magnetization measurements. Neutron diffraction measurements are reported in the temperature range 1.5−293 K for $TbCr_2Si_2$, 1.5−718 K for $HoCr_2Si_2$ whilst measurements at 2 K and 100 K are reported for $ErCr_2Si_2$. These comprehensive results show that the Cr sublattice orders anti-ferromagnetically in RCr_2Si_2 compounds with Néel temperatures above 700 K. The rare earth sublattice orders independently of the Cr sublattice, but only at low cryogenic temperatures and even at such temperatures long range order is not fully achieved for compounds with Tb and Ho, as evidenced by the present neutron diffraction data which show the presence of diffuse magnetic intensity at 1.5 K for $TbCr_2Si_2$ and $HoCr_2Si_2$. In contrast, the Er sublattice in $ErCr_2Si_2$ orders ferromagnetically just below 2.4 K

2 Sample preparation and experimental methods

Samples of RCr_2Si_2 (R = Tb, Ho and Er) were prepared by arc melting starting materials of at least 3N purity. The resulting ingots were then wrapped in Ta foil, sealed in an evacuated quartz tube and annealed for three weeks at 700 °C. X-ray diffraction measurements showed that the samples were single phase, with the exception of $ErCr_2Si_2$, where the impurity phases Er_2O_3 (0.5 at %), Cr_5Si_3 (8.0 at %) and $ErSi_x$ (10.6 at %) were identified. The RCr_2Si_2 phases crystallize in the tetragonal $ThCr_2Si_2$ structure, with all observed reflections satisfying the condition $h + k + l = 2n$ (space group I4/mmm.) Neutron powder diffraction measurements were performed on the multi-detector powder diffractometers E9 and E6 located at the BER II reactor, Berlin Neutron Scattering Centre, Hahn Meitner Institute, Germany. Data were collected in the temperature range from 1.2 K to 713 K. The angular range of 2θ was from 20 to 98 degrees using an incident neutron wavelength of 1.79636 Å, obtained from the (511) reflection of a Ge monochromator for the E9 diffractometer, whilst an incident wavelength of 2.447 Å, with data collected in the angular range of 5 to 105 degrees, was employed on the E6 diffractometer. Approximately 25 g of material were used in the neutron diffraction experiments. Magnetic ordering temperatures were determined by DSC measurements on a Perkin-Elmer DSC-7 system using the peak in the heat capacity as the signature of magnetic ordering. The heating rate used was 40 K/minute, using 22 mg of sample. Standard magnetic susceptibility measurements (H = 100 A/m) were carried out over the temperature range 4.2−300 K using a Quantum Design SQUID magnetometer.

The neutron diffraction data reported here were analyzed by the Rietveld technique [13], using the FULLPROF package for refinement of crystal and magnetic structures by constant wavelength neutron powder diffraction [14]. The magnetic form factors for metallic Cr and trivalent Er were employed in the neutron profile refinement [15]. Neutron nuclear scattering lengths of $b_{\mathrm{Tb}} = 0.738 \times 10^{-12}$ cm, $b_{\mathrm{Ho}} = 0.801 \times 10^{-12}$ cm , $b_{\mathrm{Er}} = 0.779 \times 10^{-12}$ cm, $b_{\mathrm{Cr}} = 0.775 \times 10^{-12}$ cm and $b_{\mathrm{Si}} = 0.458 \times 10^{-12}$ cm were employed in the refinement [16]. Parameters varied included a scale factor, tetragonal lattice cell constants and the positional parameter z for the Si atom. In the final stages of each refinement, an overall isotropic Debye Waller parameter for the rare earth, Cr and Si atoms as well as the Cr and Er magnetic moments, were varied. The determination of the magnetic ordering modes of the Er and Cr sublattices is based on the method of representation analysis [17,18] and employed the *SARA*h program [19].

3 Results and analysis

3.1 Magnetic ordering of RCr_2Si_2

The observed reflections in the neutron powder diffraction patterns show the same behaviour as reported previously for $HoCr_2Si_2$ in the temperature range 1.6−293 K [12] and a preliminary analysis of the measured neutron diffraction patterns reported here indicated that the intensities of peaks such as (101), (103) and (211) are again markedly different from those expected for the tetragonal $ThCr_2Si_2$ structure. This structure consists of rare earth and Cr atoms at the special positions 2a and 4d respectively, whilst Si atoms reside at 4e (00z) sites, with $z \sim 0.38$. The (101) reflection in particular has a very small calculated nuclear structure factor for neutrons. The observed intensity of the (101) peak is much greater than that calculated for a purely nuclear contribution. The temperature dependence of the low angle sections of the neutron diffraction patterns measured for $TbCr_2Si_2$ and $HoCr_2Si_2$, are shown in Figures 1 and 2 respectively. The intensity of the (101) reflection is strongly temperature dependent. For example, in the temperature range 293 K to 675 K the intensity of this reflection, observed for $HoCr_2Si_2$, decreases by a factor of 12, as displayed in Figure 3. The origins of this peak and others such as (103) and (211) clearly reside in the magnetic ordering of the Cr sublattice, whilst the Tb and Ho sublattices possibly order only at very low cryogenic temperatures. This is demonstrated by the presence of broad reflections at low angles for both $TbCr_2Si_2$ and $HoCr_2Si_2$. The diffraction patterns

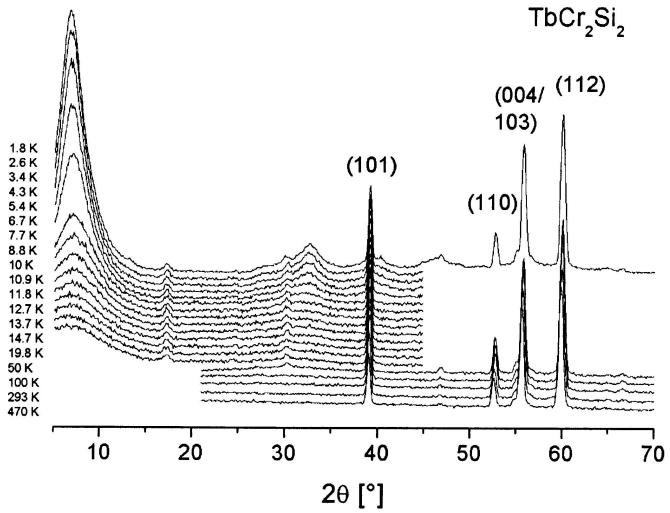

Fig. 1. A section of the observed neutron diffraction pattern for $TbCr_2Si_2$ in the temperature range 1.8−470 K (incident neutron wavelength 2.447 Å).

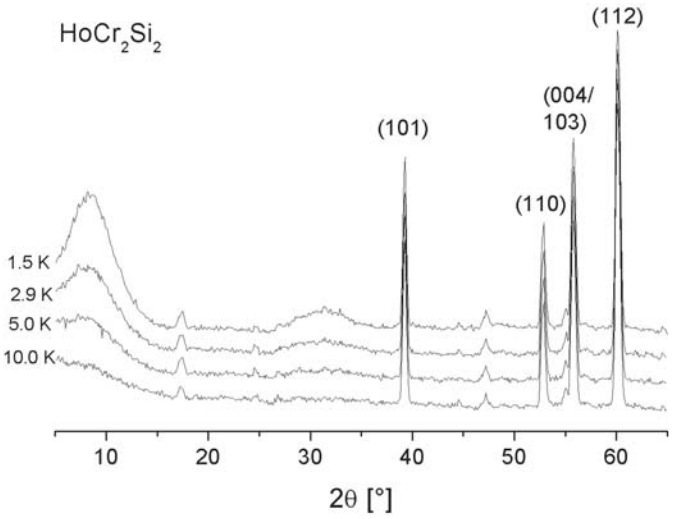

Fig. 2. A section of the observed neutron diffraction pattern for $HoCr_2Si_2$ in the temperature range 1.5−10 K (incident neutron wavelength 2.447 Å).

for $TbCr_2Si_2$ below around 20 K show the build up of diffuse magnetic intensity centred at scattering angles 7 and 32°. The appearance of this intensity could be associated with a short range ordering of the R sublattice, the onset of which takes place independently of the Cr sublattice. However, the fact that the diffuse magnetic peaks are still broadened at $T \sim 1.5$ K shows that any presumable long range magnetic ordering of the rare earth sublattice is not fully achieved even at such a low temperature. Rather, it could be associated with a short range ordering. This is seen in the temperature dependence of the intensity of the first diffuse peak and its associated full width at half height maximum (FWHM), which is displayed in Figure 4 for $TbCr_2Si_2$.

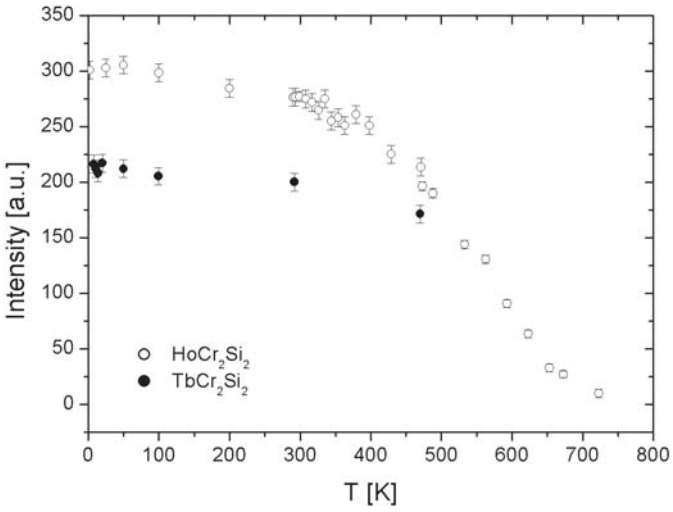

Fig. 3. Temperature dependence of the integrated intensity of the (101) reflection for $HoCr_2Si_2$ and $TbCr_2Si_2$.

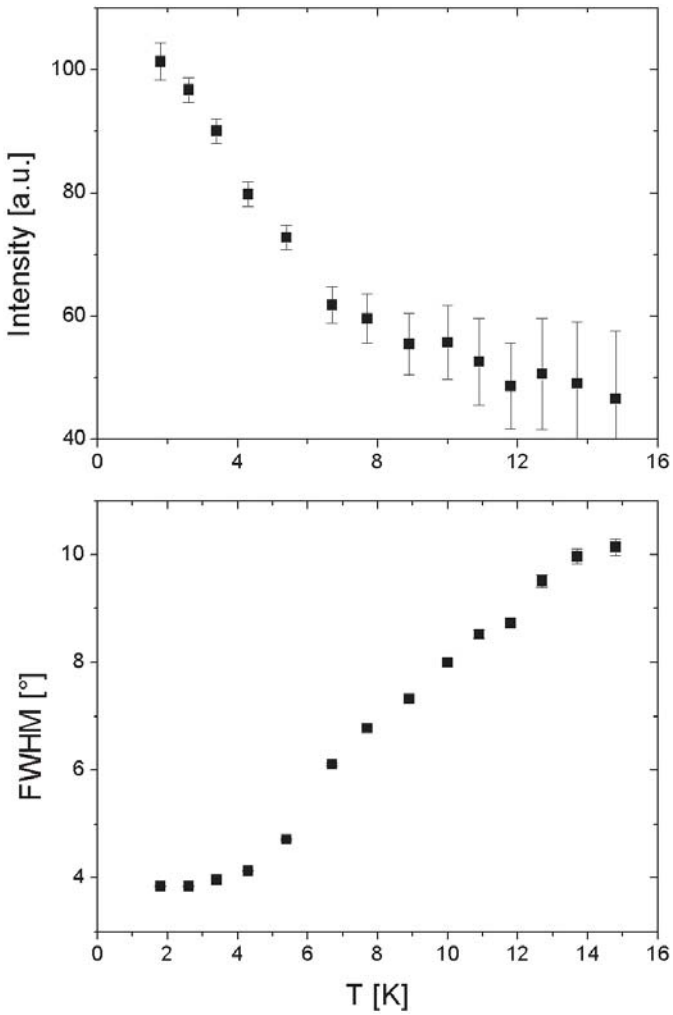

Fig. 4. Temperature dependence of the integrated intensity and FWHM of the low angle diffuse peak for $TbCr_2Si_2$.

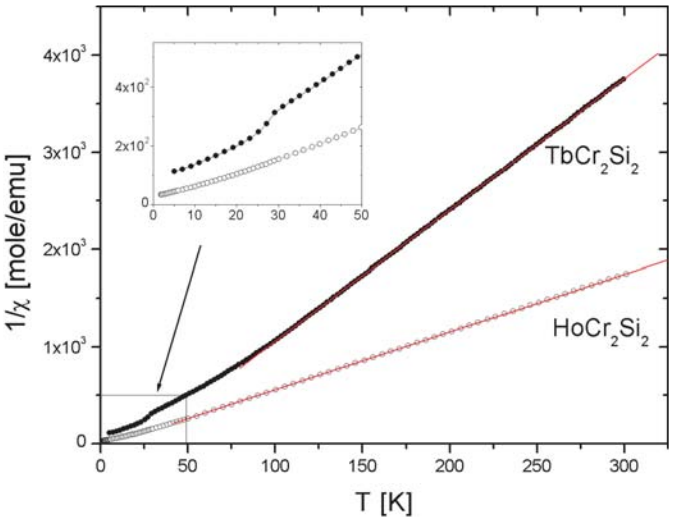

Fig. 5. Temperature dependence of the reciprocal susceptibility for $TbCr_2Si_2$ and $HoCr_2Si_2$.

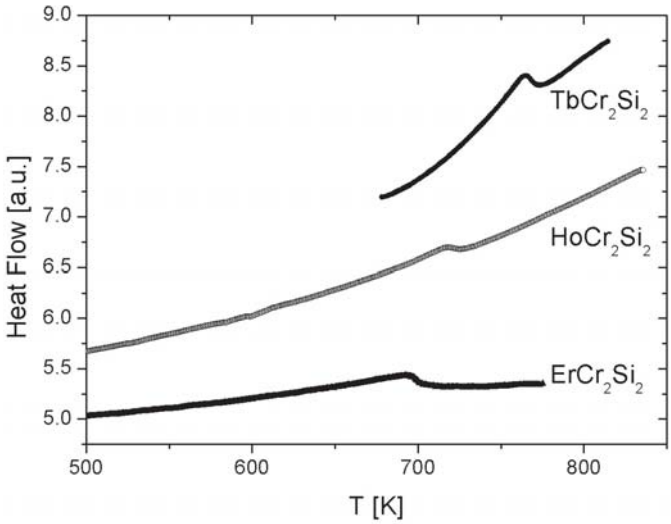

Fig. 6. Differential Scanning Calorimetry data for RCr_2Si_2 (R = Tb, Ho and Er.)

The temperature dependence of the susceptibility for $TbCr_2Si_2$ and $HoCr_2Si_2$ is displayed in Figure 5. Above 100 K the susceptibility for $TbCr_2Si_2$ appears to display Curie-Weiss dependence. We therefore fitted the susceptibility data above 100 K for this compound with the Curie-Weiss expression $\chi = C/(T-\Theta)$, yielding a paramagnetic Curie temperature of $\Theta = -2.6$ (2) K. At a temperature of approximately 25 K a small kink in the plot of $1/\chi\,(T)$ is evident and indicates a possible triggering of magnetic ordering for the Tb sublattice. No such ordering signal was detected in the susceptibility of $HoCr_2Si_2$.

A similar situation as in $TbCr_2Si_2$ is observed in the neutron diffraction patterns of $HoCr_2Si_2$, with a build up of magnetic diffuse intensity centred at scattering angles of 7 and 32 degrees ($Q \sim 0.34$ Å^{-1} and 1.33 Å^{-1} respectively) but in this instance any onset of magnetic order must occur at lower temperatures than observed for $TbCr_2Si_2$. In contrast to the Tb and Ho compounds, $ErCr_2Si_2$ shows no short range ordering at low temperatures. The neutron diffraction data obtained for $ErCr_2Si_2$ confirm that the magnetic ordering of the Er sublattice is complete at 1.6 K. We attribute this effect to a magnetic crystal field ground state.

3.2 Magnetic order of the Cr sublattice

The Differential Scanning Calorimetry results for all three compounds RCr_2Si_2 (R = Tb, Ho and Er) are displayed in Figure 6 and clearly show a small peak at 758 K for $TbCr_2Si_2$, 718 K for $HoCr_2Si_2$ and 692 K for $ErCr_2Si_2$. These can be taken as a signature of the antiferromagnetic ordering of the Cr sublattice for each compound.

The magnetic reflections from the long-range-ordered magnetic state of the Cr sublattice observed in the neutron diffraction patterns of all three RCr_2Si_2 compounds obtained above ∼25 K obey the reflection condition $h+k = 2n+1$, which corresponds to an 'anti-C' centring translation mode in which Cr atoms at the positions $(0, 1/2, 1/4)$ and $(1/2, 0, 1/4)$ have anti-parallel magnetic moments. Associated with each of these two sites is the body centring translation $+(1/2, 1/2, 1/2)$ and the corresponding magnetic structure factor, in units of 10^{-12} cm, for the observed reflections can thus be written as:

$$F(hkl) = 0.27 f(hkl) \left[\exp \pi i \left(h + \frac{l}{2}\right) - \exp \pi i \left(k + \frac{l}{2}\right)\right] \times [1 + \cos \pi\,(h+k+l)] \quad (1)$$

where $f(hkl)$ is the magnetic form factor for Cr (there is no nuclear contribution to the intensity of peaks with $h + k = 2n + 1$ from the Cr atoms). In this particular instance, the magnetic structure of the Cr sublattice in RCr_2Si_2 compounds consists of Cr atoms with an AF (anti-ferromagnetic) coupling to atoms at first NN (Nearest Neighbour) positions, ferromagnetic at second NN and AF at third NN. In the framework of a mean field – RPA (Random Phase Approximation) model, such a magnetic structure is indeed stabilized for values of $h + k = 2n + 1$. (See Appendix.)

The possible configurations of magnetic moments at the Cr 4d sites in the space group I4/mmm, together with the basis vectors of the irreducible representations Γ_i for these sites, were determined by representation analysis. There are 16 symmetry operators, combined with the I translation $+(1/2, 1/2, 1/2)$ in the I4/mmm space group and the underlying point group 4/mmm has 10 irreducible representations, 8 of which are one-dimensional ($\Gamma_1 \ldots \Gamma_8$) and 2 are two-dimensional (Γ_9 & Γ_{10}). The Cr atoms reside at the 4d site $(0\,1/2\,1/4)$ with the point group $\bar{4}$m2. Our neutron diffraction data show that the Cr sublattice orders antiferromagnetically along the c-axis [001] with anti-C ordering. The Cr moments at $(0, 1/2, 1/4)$ and $(1/2, 0, 1/4)$ are antiparallel and the moments related by the

Table 1. Representations and basis vectors for the Cr and R sites in RCr_2Si_2 (space group I4/mmm).

Representation	Basis vectors [Cr atoms at (0 1/2 1/4) and (1/2 0 1/4)]
Γ_3	$\Psi_1 = +z$ and $+z$ [one-dimensional representation]
Γ_6	$\Psi_2 = +z$ and $-z$ [one-dimensional representation]
Γ_9	$\Psi_3 = x - iy \,\&\, x - iy$ [two-dimensional representation]
	$\Psi_4 = x + iy \,\&\, x + iy$
Γ_{10}	$\Psi_5 = x + iy \,\&\, -x - iy$ [two-dimensional representation]
	$\Psi_6 = -x + iy \,\&\, x - iy$

Representation	Basis vectors [R atom at (0 0 0)]
Γ_3	$\Psi_1 = +z$ [one-dimensional representation]
Γ_9	$\Psi_2 = x - iy$ [two-dimensional representation]
	$\Psi_3 = x + iy$

$+(1/2,\ 1/2,\ 1/2)$ translation are parallel. For a propagation vector $\mathbf{k} = [000]$, the decomposition of the magnetic representation for the Cr 4d-site in RCr_2Si_2 is $\Gamma_3 \oplus \Gamma_6 \oplus \Gamma_9 \oplus \Gamma_{10}$ and the corresponding basis vectors are as tabulated in Table 1. The observed magnetic ordering of the Cr sublattice along the c-axis [001] with the anti-C order corresponds to the one-dimensional magnetic representation Γ_6. Within this representation, the characters of the generating operators 4_Z, m_Z, m_X and m_{XY} in the point group 4/mmm are -1, -1, -1 and $+1$ respectively, which correspond to the magnetic space group I4′/m′ m′ m [20]. The results of the refinement of the magnetic structures, in the magnetic space group I4′/m′ m′ m, for $TbCr_2Si_2$ and $HoCr_2Si_2$ at 293 K are shown in Figure 7. The temperature dependence of the refined magnetic moments of the Cr sublattice for $TbCr_2Si_2$ and $HoCr_2Si_2$ are displayed in Figure 8 (for completeness, this figure also displays neutron diffraction results previously reported in the low temperature region from 1.6 to 293 K for $HoCr_2Si_2$).

The magnetic moment mode for the Cr sublattice which best agrees with our neutron diffraction data is G_Z (representation Γ_6) which corresponds to a $(+\ -\ +\ -)$ sequence of moment orientations within a given (001) Cr plane, and for the compounds presented here, the Cr magnetic mode for the four spins S_i at the 4d sites within a (001) plane is therefore:

$$G_z = S_{1z} - S_{2z} + S_{3z} - S_{4z} \qquad (2)$$

with the subscript denoting the ordering direction, which in this case is along [001]. The relative orientation between adjacent Cr planes, e.g. at $z = 1/4$ and $z = 3/4$, is given by the observation that Cr moments related by the $+(1/2, 1/2, 1/2)$ I-translation are parallel. Alternatively, we may consider the unit cell grouping of Cr atoms at the

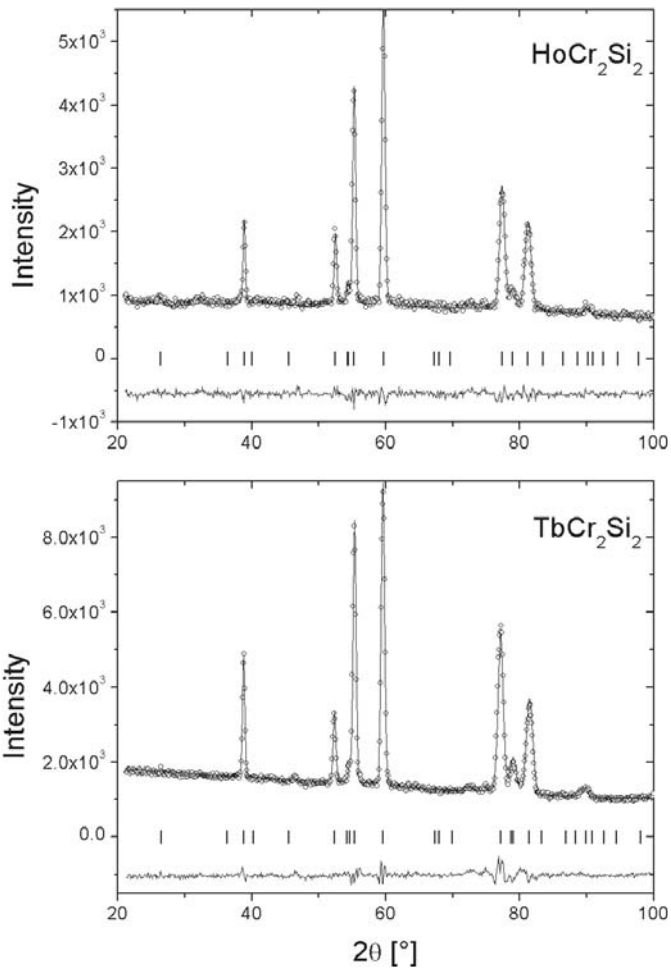

Fig. 7. Observed, calculated and difference neutron diffraction patterns for $TbCr_2Si_2$ and $HoCr_2Si_2$ measured at 293 K. Tick-marks include nuclear and magnetic reflections (incident neutron wavelength 2.447 Å).

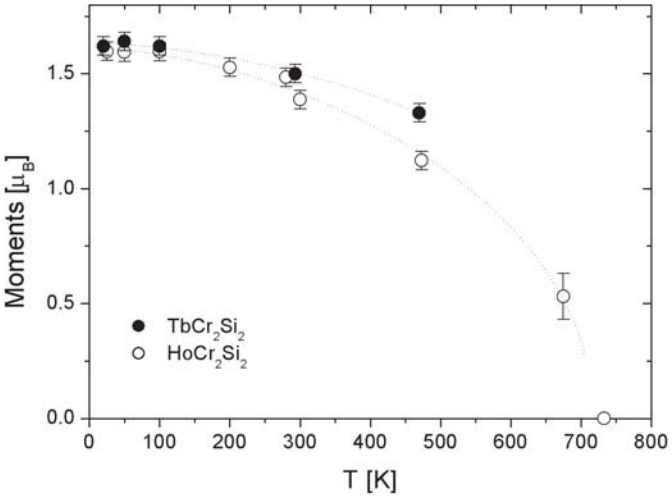

Fig. 8. Temperature dependence of the refined Cr magnetic moment for $TbCr_2Si_2$ and $HoCr_2Si_2$ (for completeness, this figure also includes neutron diffraction results previously reported in the low temperature region from 1.6 to 293 K for $HoCr_2Si_2$[12].) The dotted line is only a guide to the eye.

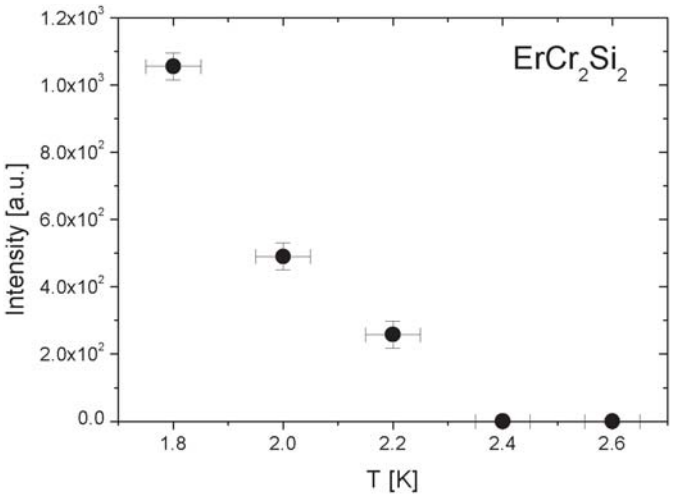

Fig. 9. Temperature dependence of the integrated intensity of the (002) reflection for $ErCr_2Si_2$.

4d positions $(0, 1/2, 1/4)$, $(1/2, 0, 1/4)$, $(1/2, 0, 3/4)$ and $(0, 1/2, 3/4)$ which also exhibits the G_Z magnetic mode.

3.3 Magnetic order of the Er sublattice

The Er 2a site (0,0,0) has the point group $4/mmm$. The Erbium moments in $ErCr_2Si_2$ order independently of the Cr sublattice at a temperature two orders of magnitude lower than the Cr sublattice Néel temperature. From the temperature dependence of the (002) reflection for $ErCr_2Si_2$, as displayed Figure 9, we deduce that Er orders ferro-magnetically below 2.4 K. For a propagation vector $\mathbf{k} = [000]$, the decomposition of the magnetic representation for the Er 2a site is $\Gamma_3 \oplus \Gamma_9$ and the corresponding basis vectors are as shown in Table 2. The Γ_3 representation, coupled with the propagation vector $\mathbf{k} = [000]$ would yield a ferromagnetic alignment of the two Er moments along [001]. Experimentally, we observe that the Er order is ferromagnetic with the Er moments in the basal plane; the observation of a magnetic contribution from the Er sublattice to the (002) peak precludes c-axis order. Hence, the magnetic representation describing the magnetic order of the Er sublattice is the two-dimensional Γ_9 representation. The magnetic ordering of the Er sublattice is therefore a linear combination of the Ψ_2 and Ψ_3 basis vectors. Within the two-dimensional Γ_9 representation, the characters of the generating operators 4_Z, m_Z, m_X and m_{XY} are $0, -2, 0$ and 0 respectively. Using the Γ_9 representation of the magnetic structure for the Er sublattice in $ErCr_2Si_2$, the observed and calculated diffraction patterns at 2 K and 100 K are displayed in Figure 10. The magnetic moment of Er is aligned within the basal plane and at 1.8 K we obtain a moment of $\mu_{\mathrm{Er}} = 5.24\ (5)\ \mu_B$.

The results of refinements of the structural and magnetic moment parameters for $TbCr_2Si_2$, $HoCr_2Si_2$ and $ErCr_2Si_2$ at 100 K and for $ErCr_2Si_2$ at 2 K are presented in Table 2 whilst the magnetic structure of the Cr and Er sublattices in RCr_2Si_2 compounds, as determined in the present investigation, is displayed in Figure 11.

4 Discussion and conclusion

The magnetic ordering of the Cr sublattice in $ThCr_2Si_2$ type compounds has remained, until now, undetected in previously reported magnetization measurements. The conclusive neutron diffraction measurements reported here improve significantly the cycle of our knowledge of the magnetic interactions of the transition metal sublattice in the important and highly documented RT_2Si_2 series with T = Mn, Fe, Ni, Cr. In compounds of the type RFe_2Si_2 and RNi_2Si_2, the Fe and Ni sublattices do not order magnetically. However, in contrast to RMn_2Si_2 compounds which display competing Mn-Mn anti-ferromagnetic and ferromagnetic interactions, no similar effects appear to be at work in RCr_2Si_2 compounds. In RMn_2Si_2 compounds, an anti-ferromagnetic coupling within (001) Mn planes is observed when interlayer Mn-Mn distances are greater than a critical distance of about 2.87 Å. In addition, there is a strong dependence of the ordering temperatures on the interlayer distances for RMn_2X_2 compounds [21]. The corresponding Cr–Cr interlayer distance in RCr_2Si_2 is smaller, about 2.75 Å, and we associate this small distance with an unexpectedly large ordering temperature and associated large magnetic moment of the Cr sublattice.

Electronic band structure calculations on RT_2X_2 compounds, for T = Mn, Fe, Ni and Co are in overall agreement with the experimentally observed magnetic phenomena for these compounds. Compounds with T = Mn obey

Table 2. Results of Rietveld profile refinements of neutron diffraction data obtained at 100 K for $TbCr_2Si_2$, $HoCr_2Si_2$ and $ErCr_2Si_2$ where only the Cr sublattice is magnetic. In addition, we include the results of the refinement of the 2 K pattern of $ErCr_2Si_2$ at which temperature both the Er and Cr sublattices are magnetically ordered. Errors refer to Estimated Standard Deviations calculated by Rietveld refinement (a typical detection limit of μ_B for neutron powder diffraction is $\pm$ 0.15μ_B. Observed and calculated neutron intensities and structure factors for all three compounds are available on request from the authors.

	$TbCr_2Si_2$	$HoCr_2Si_2$	$ErCr_2Si_2$	$ErCr_2Si_2$
T (K)	100	100	100	2
a (Å)	3.9103(5)	3.8931(1)	3.8954(4)	3.8950(2)
c (Å)	10.619(1)	10.6109(2)	10.633(2)	10.632(1)
z/c, Si (4e)	0.3861(3)	0.3854(3)	0.3888(4)	0.3888(4)
B_{ov}(Å^2)	0.5(2)	0.20(4)	0.5(2)	0.25 (fixed)
μ_B, Cr	1.62(2) $\parallel c$	1.60(4) $\parallel c$	1.41(3) $\parallel c$	1.35(7) $\parallel c$
μ_B, Rare-earth	–	–	–	5.24(5) $\perp c$
R_{wp}, %	3.90	8.61	5.14	7.20
R_{exp}, %	2.08	5.24	3.45	3.47
χ^2	3.5	2.70	2.21	4.29

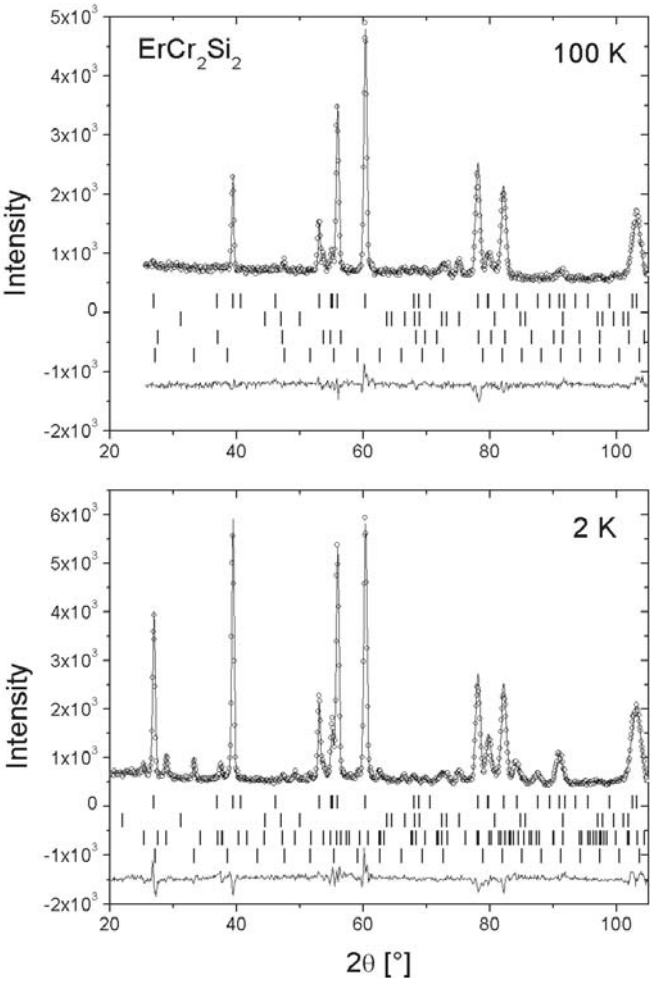

Fig. 10. Observed, calculated and difference neutron diffraction patterns for $ErCr_2Si_2$ at 2 and 100 K. Tick-marks include nuclear and magnetic reflections of the main and impurity phases (from top to bottom: $ErCr_2Si_2$, Cr_5Si_3, ErSi and Er_2O_3).

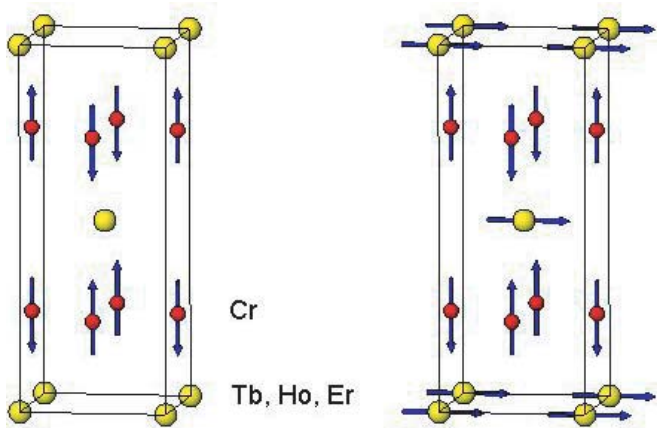

Fig. 11. Left: Schematic of the crystal and magnetic structure of the Cr sublattice for RCr_2Si_2 compounds (R = Tb, Ho, Er.) For clarity only the rare earth (large symbol) and Cr atoms (small symbol) are shown. Right: The magnetic structure of Er and Cr sublattices in $ErCr_2Si_2$ at 1.8 K.

the Stoner criterion for magnetic ordering, whilst compounds with, for example T = Co, do not fulfil this criterion [22]. In light of the results presented here we can anticipate similar computations for the RCr_2Si_2 series. The measurements reported here together with those planned for the RCr_2Ge_2 series, should establish whether the dependence of the Cr-Cr exchange interactions on the interlayer Cr-Cr distance is as sensitive to the interlayer distance as observed in RMn_2X_2 (X = Si, Ge) compounds.

Finally, the presence of magnetic diffuse scattering observed at low temperatures for $TbCr_2Si_2$ and $HoCr_2Si_2$ clearly demonstrates that Tb and Ho moments are not yet fully ordered, even in the presence of a large Cr exchange field. This is most likely due to a non-magnetic singlet crystal field ground state, as determined by inelastic neutron scattering measurements on $HoCr_2Si_2$ which

report a singlet Γ_1 crystal field ground state for the Ho^{3+} ion [10]. We therefore attribute the magnetic behaviour of the R sublattice in these three compounds to a crystal field induced frustration, associated with the non magnetic singlet for Tb and Ho and magnetic doublet ground states for the Er ion.

Financial support by the Italian MURST National Research Program "Alloys and Intermetallic Compounds: Thermodynamics, Physical Properties, Reactivity, is gratefully acknowledged. Financial assistance from the EC-IHP program for participation in the neutron diffraction experiment at HMI is gratefully acknowledged. J.M. Cadogan is grateful to the Australian Research Council, Australian Nuclear Science and Technology Organisation and the Australian Academy of Science for financial support.

Appendix

The proposed magnetic structure of the Cr sublattice in RCr_2Si_2 compounds can be expressed in terms of the Fourier transform of respective antiferromagnetic and ferromagnetic exchange interactions between first, second and third nearest neighbours of a Cr atom. The Fourier transform is [23]:

$$J(\vec{q}) = \sum_{R,R'} J(\vec{R} - \vec{R}') \cos\{\vec{q} \cdot (\vec{R} - \vec{R}')\} \qquad (3)$$

where $\vec{q}$ is a magnetic reciprocal wave-vector and J $(\vec{R}-\vec{R}')$ represents the exchange interaction between atoms separated by a distance $R - R'$. For the body centred tetragonal lattice under consideration and nominally placing a Cr atom at the origin $\vec{R} = (0, 0, 0)$ with a spin (+) and considering the G_z^- basis of the irreducible representation for the magnetic structure, there are four Cr atoms at first NN positions: $\left(\frac{a}{2}, \frac{a}{2}, 0\right)$, $\left(-\frac{a}{2}, -\frac{a}{2}, 0\right)$, $\left(\frac{a}{2}, -\frac{a}{2}, 0\right)$ $\left(-\frac{a}{2}, \frac{a}{2}, 0\right)$ with spin (−), four second NN atoms at (a, 0, 0), $(-a, 0, 0)$, $(0, a, 0)$, $(0, -a, 0)$ with (+) spin and finally two third NN atoms at positions with $\left(0, 0, \frac{c}{2}\right)$, $\left(0, 0, -\frac{c}{2}\right)$ with spin (−) (lattice parameters of the crystal lattice are denoted by a and c). With this definition of the magnetic lattice, the Fourier transform $J(\vec{q})$ reduces to:

$$J(\vec{q}) = 4J(R_1)\left[\cos\left(\frac{q_x a}{2}\right)\cos\left(\frac{q_y a}{2}\right)\right] + 2J(R_2)\left[\cos(q_x a) + \cos(q_y a)\right] + 2J(R_3)\cos\left(\frac{q_z c}{2}\right) \qquad (4)$$

with $\vec{q} = (q_x, q_y, q_z)$. In the mean field – Random Phase Approximation, the wave-vector dependent susceptibility diverges at the Néel point for values of $\vec{q}$ which maximize $J(\vec{q})$. The magnetic structure is thus stabilized for values of q_x, q_y, and q_z which satisfy the conditions:

$$\left(\frac{\partial J(q)}{\partial q_i}\right) = 0 \qquad (5)$$

$(i = x, y, z.)$ With reference to the Cr sublattice in RCr_2Si_2, the smallest value of q in this instance is thus given by the magnetic reciprocal lattice vector $q = (1, 0, 1)$. This value corresponds to the first magnetic reflection (101) observed in the neutron diffraction pattern. For this value of q, $J(1, 0, 1) = -4J(R_1) + 4J(R_2) - 2J(R_3)$. Other magnetic peaks are also observed in the neutron diffraction pattern, for example the (1,0,3) and (2,1,1) reflections. These values of q give the same value for J as $J(1, 0, 1)$.

References

1. A. Szytula, in *Handbook of Magnetic Materials*, Vol. **6**, Elsevier, Amsterdam, edited by K.H.J. Buschow (Elsevier, 1991), pp. 87 –179
2. M. Sikirica, Z. Ban, Acta Cryst. **18**, 594 (1965)
3. Z. Ban, M. Sikirica, Croat. Chem. Acta **36**, 151 (1964)
4. Z. Ban, L. Omejec, A. Szytula, Z. Tomkowicz, Phys. Stat. Solidi (a) **27**, 333 (1975)
5. M. Hofmann, S.J. Campbell, S.J. Kennedy, X.L. Zhao, J. Magn. Magn. Mater. **176**, 279 (1997)
6. H. Pinto, H. Shaked, Phys. Rev. B **7**, 3261 (1973)
7. A. Dommann, F. Hulliger, Ch. Baerlocher, J. Less-Common Metals **147**, 97 (1988)
8. M.W. Dirken, R.C. Thiel, K.H.J. Buschow, J. Less-Common Metals **147**, 97 (1989)
9. R. Coehoorn, K.H.J. Buschow, M.W. Dirken, R.C. Thiel, Phys. Rev. B **42**, 4645 (1990)
10. O. Moze, S. Rosenkranz, R. Osborn, K.H.J. Buschow, J. Appl. Phys. **87**, 6283 (2000)
11. I. Ijjaali, G. Venturini, B. Malaman, J. Alloys and Compounds **279**, 102 (1998)
12. O. Moze, M. Hofmann, K.H.J. Buschow, J. Alloys and Compounds **308**, 60 (2000)
13. H.M. Rietveld, J. Appl. Crystallogr. **2**, 65 (1969)
14. J. Rodriguez-Carvajal, Physica B **192**, 5 (1993). The FULLPROF manual and PC version of the FULLPROF refinement program are obtainable from the Laboratoire Leon Brillouin web site, `http://www-llb.cea/fr`
15. E.J. Lisher, J.B. Forsyth, Acta Cryst. A **27**, 545 (1971)
16. V.F. Sears, Neutron News **3**, 26 (1992)
17. E.F. Bertaut, in *Treatise on Magnetism*, edited by H. Suhl, G.T. Rado, Vol. III, Chap. 4 (New York Academic Press, 1965), p. 149
18. E.F. Bertaut, Acta Cryst. A **24**, 217 (1968)
19. A.S. Wills, Physica B **276**, 680 (2000); program available from `ftp://ftp.ill.fr/pub/dif/sarah/`
20. W. Opechowski, R. Guccione, in *Treatise on Magnetism*, edited by H. Suhl, G.T. Rado, Vol. IIA, Chap. 3 (New York Academic Press, 1965), p. 105
21. A. Szytula, J. Alloys and Compounds **178**, 1 (1992)
22. S. Ishida, S. Asano, J. Ishida, J. Phys. Soc. Jpn **55**, 93 (1986)
23. J.S. Smart, in *Effective Field Theories of Magnetism* (Saunders, Philadelphia, 1966)